Acc. Chem. Res. 1988, *21*, 250–254

Nickel Dibromide: A Magnetic Detective Story

PETER DAY

Inorganic Chemistry Laboratory, Oxford University, South Parks Road, Oxford OX1 3QR, England

Received July 21, 1987 (Revised Manuscript Received March 16, 1988)

Ferro- and antiferromagnetism are the commonplace types of long-range magnetic order in inorganic solid-state chemistry. The first occurs in a lattice containing localized moments, for example arising from unpaired d or f electrons, when the interaction between neighboring (n) moments, measured by the exchange constant J_n, is such as to couple them parallel. At low temperatures, when thermally induced disorder cannot disrupt the near-neighbor interactions, the free energy of the ensemble of moments is minimized when they are all parallel, and the magnetization of the whole lattice is saturated. Conversely, when the interaction between near neighbors couples them antiparallel, there is no net moment in zero field at low temperature. In any real lattice, though, there are not only the immediate neighbors of a magnetic ion to be considered, but next nearest (nn), next next nearest (nnn), etc. Clearly, if the interactions between all these are ferromagnetic, the long-range order must be ferromagnetic. What, though, if the (n) interaction is ferromagnetic (J_n positive) and the (nn) and (nnn) are antiferromagnetic (J_{nn} and J_{nnn} negative)?

Fortunately this problem does not arise very often in ionic lattices because the unpaired electrons are quite firmly localized onto individual cations and J_n dominates J_{nn}, even if there are more (nn) than (n). Nevertheless, occasionally the metal–ligand covalency combined with a favorable lattice topology may be sufficient to strengthen the (nn) superexchange to the point where it begins to compete with J_n in determining the long-range order. Such a case, occurring in the simple binary compound $NiBr_2$, is the subject of this Account.

$NiBr_2$ has a simple layer structure isomorphous with $CdCl_2$, but it turns out that because of competition between ferromagnetic J_n and antiferromagnetic J_{nn} and J_{nnn}, its magnetic ordering is highly unusual. In fact it changes from a collinear structure to an incommensurate helical one with decreasing temperature and moreover with a helix repeat length that varies with temperature and pressure. This Account is also a detective story, since the indicators for the existence of unusual magnetic order were at first indirect. Evidence from a variety of physical methods has to be combined to produce a coherent picture of the ordering process. In particular optical spectroscopy and neutron scattering were employed to measure the magnetic phase diagram and interpret the unique magnetic behavior. Chemical substitution was also used extensively to probe the effect of varying the electron configuration of the transition-metal ion and the nature of the anions bridging between them.

Noncollinear Magnetic Structures

The simplest example of a magnetic structure whose periodicity differs from that of the nuclear structure is the two-sublattice antiferromagnet. A relevant example is provided by the transition-metal dihalides exhibiting the $CdCl_2$ or CdI_2 layer structures. These were dubbed metamagnetic by Landau[1a] because despite being antiferromagnetic below their ordering temperatures, they may be ferromagnetically saturated above a relatively small critical magnetic field applied in the *ab* plane (CoX_2, NiX_2) or parallel to the *c* axis (FeX_2). Landau proposed a model in which moments are ferromagnetically aligned within the *ab* plane, either parallel or perpendicular to the *c* axis, with weak antiferromagnetic coupling between adjacent planes. This was subsequently confirmed by neutron diffraction.[1b]

Figure 1 displays the $CdCl_2$ structure of $NiBr_2$, clearly showing that exchange between neighboring ions within each layer (J_n) occurs via a single bridging halide ion whereas interlayer exchange (J') occurs via two bridging halide ions. The latter is expected to be very much smaller in magnitude, thus explaining the observed predominantly two-dimensional magnetism. Figure 1 also illustrates how the (n), (nn), and (nnn) pairs of metal ions within the layers are coupled by J_n, J_{nn}, and J_{nnn}.

More complex antiferromagnetic structures can arise where there is competition between magnetic interactions that favor the alignment of magnetic moments in different directions in the lattice.[2] Five separate types of competiton have been identified. First, there may be competing exchange interactions between a magnetic species and its first and further crystallographically equivalent nearest-neighbor shells. Second, competing exchange interactions may occur between a magnetic species and its nearest neighbors, if they occupy crystallographically inequivalent sites. Third, there could be competition in exchange involving different magnetic species. Fourth, in metallic systems competing long-range exchange interaction can take place via the conduction electrons, and itinerant exchange between the conduction electrons themselves, and finally competition is set up between exchange and dipolar interactions, when the former are very weak.

In low-dimensional magnetic materials, it is easier to identify the sources of competing interactions because such interactions are fewer in number. $NiBr_2$,[3] NiI_2,[4]

Peter Day received his D.Phil. from Oxford University in 1965 for work initiating the modern-day study of mixed-valency compounds. He worked with C. K. Jorgensen at the Cyanamid Institute in Geneva, Switzerland, and briefly at Bell Laboratories, Murray Hill, NJ. Since 1967 he has been a lecturer in Inorganic Chemistry at Oxford University and Fellow of St. John's College. He received the Corday–Morgan Medal of the Royal Society of Chemistry in 1971 and their Award for Solid State Chemistry in 1986. In 1986 he was elected a Fellow of the Royal Society.

(1) (a) Landau, L. D. *Phys. Z. Sowjetunion* **1933**, *4*, 675. (b) Wilkinson, M.; Cable, J. W.; Wollan, E. O.; Koehler, W. C. *Phys. Rev.* **1959**, *113*, 497.

(2) Villain, J. *J. Phys. Chem. Solids* **1959**, *11*, 303.

(3) Day, P.; Dinsdale, A. T.; Krausz, E. R.; Robbins, D. J. *J. Phys. C* **1976**, *9*, 2481.

(4) Kuindersma, S. R.; Sanchez, J. P.; Haas, C. *Physica B* **1981**, *111B*, 231.

0001-4842/88/0121-0250$01.50/0

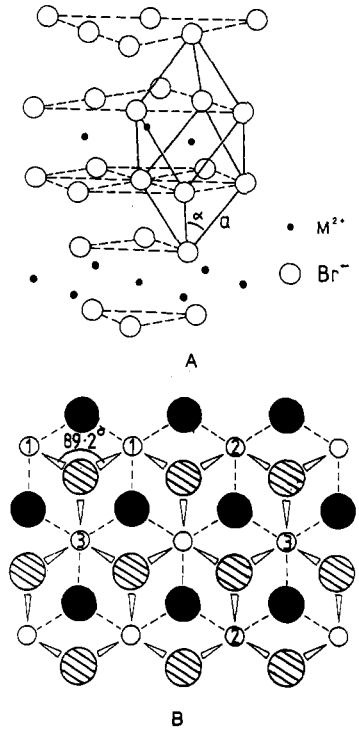

Figure 1. (A) Elevation and (B) plane view of the crystal structure of $NiBr_2$; (1,1), (2,2), and (3,3) are the (n), (nn), and (nnn) pairs of cations.

and $BaCo_2(AsO_4)_2$[5] are examples of nearly two-dimensional systems where the competition is of the first type and helical magnetic phases exist. Certain members of the series of one-dimensional hexagonal perovskites $A^IB^{II}X_3$ (A = Cs, Rb; B = Fe, Mn; X = Br, Cl)[6-8] have triangular spin arrays, and the competition is essentially of the second type. Both the third and fourth types of competition also exist in magnetic insulators with the spinel ($A^{II}B^{III}{}_2O_4$) and garnet ($A^{III}{}_3B^{III}{}_2B^{III}{}_3O_{12}$) structures; for example, $MnCr_2O_4$[9] and $Ho_3Fe_2Fe_3O_{12}$[10] exhibit magnetic phases with complex spiral spin structures.

Among metals, the rare earths have long been known to show a wide variety of noncollinear magnetic phases, caused by the fourth type of competition, while HoP, which is believed to become ordered almost entirely by dipolar interactions, has a spiral magnetic phase and thus falls into the fifth category.

In most instances, a number of magnetic phase transitions take place as the temperature or applied magnetic field is raised. $NiBr_2$ is unique among the metamagnetic transition-metal dihalides, and probably among all magnetic insulators, because with decreasing temperature it undergoes a transition (at T_{IC} = 23 K) from a collinear magnetic phase to a phase with a helical modulation of the moments, and the vector describing the helical phase increases smoothly in magnitude from zero at T_{IC} to a limiting value at about 4 K.

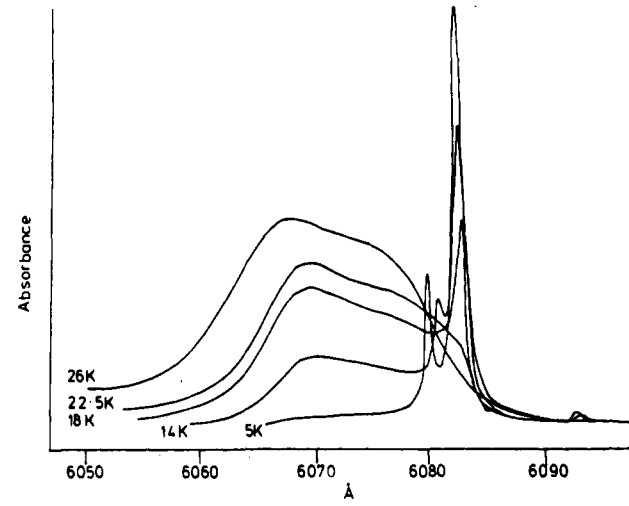

Figure 2. Temperature variation of the ligand field absorption spectra of $NiBr_2$ near 6000 Å. The cold bands are A and B.[14]

Optical Spectra

The story begins with a project on the temperature dependence of exciton–magnon absorption bands in the family of metamagnetic dihalides MX_2 (M = Mn, Fe, Co, Ni; X = Cl, Br, I).[11] In the large majority of cases J_n within the layers is ferromagnetic while the much smaller J' between layers is antiferromagnetic. Thus while the (n) interaction is ferromagnetic, the lattice as a whole is antiferromagnetic. We had already demonstrated that in purely ferromagnetic lattices, spin-forbidden ligand field transitions gain electric-dipole intensity by combining the creation of the electronic excited state (exciton) with the annihilation of thermally populated spin fluctuations (magnons).[12] The result of this mechanism is that the absorption intensity is strongly temperature dependent, disappearing at low temperature when the magnon states are no longer populated. This contrasts with the situation in purely antiferromagnetic compounds, where the exciton–magnon absorption bands become more intense with decreasing temperature.[13] The question we posed to ourselves was whether the temperature behavior of the corresponding absorption bands in the metamagnets would mimic that of a two-dimensional ferromagnet or a three-dimensional antiferromagnet.

In the event, for M = Fe, Co and X = Cl, Br, I the answer was clear: the two-dimensional ferromagnetism dominated, and "hot"-band behavior was seen.[11] In the single case of $NiBr_2$, however, not only was there a hot band in the region of the $^3A_{2g} \rightarrow {}^1A_{1g}, {}^1T_{2g}$ ligand field transition, but also next to it there were two much sharper bands that decreased rapidly in intensity with increasing temperature until at 23 K they had completely disappeared (Figure 2).[14] The widths of exciton–magnon combination bands depend on the energy dispersion of both exciton and magnon since the incoming photon creates an exciton with a wave vector **k** combined with either creation or annihilation of a magnon with a corresponding wave vector $-\mathbf{k}$.[13,15] In

(5) Regnault, L. P.; Burlet, P.; Rossat-Mignod, J. *Physica B* **1977**, *86–88B*, 660.
(6) Davidson, G. R.; Minkiewicz, V. J.; Cox, D. E.; Khattak, C. P. *AIP Conf. Proc.* **1971**, *5*, 463.
(7) Eibschuetz, M.; Sherwood, R. C.; Hsu, F. S. L.; Cox, D. E. *AIP Conf. Proc.* **1973**, *18*, 386.
(8) Wada, N.; Ubukashi, K.; Hirakawa, K. *J. Phys. Soc. Jpn.* **1982**, *51*, 2833.
(9) Hastings, K. M.; Corliss, L. M. *Phys. Rev.* **1962**, *126*, 556.
(10) Herpin, A.; Koehler, W.; Meriel, P. *Bull. Am. Phys. Soc.* **1960**, *5*, 457.
(11) Robbins, D. J.; Day, P. *J. Phys. C* **1976**, *9*, 867.
(12) For a brief review, see: Day, P. *Acc. Chem. Res.* **1979**, *12*, 236.
(13) Sell, D.; Greene, R. L.; White, R. M. *Phys. Rev.* **1967**, *158*, 489.
(14) Day, P.; Dinsdale, A.; Krausz, E. R.; Robbins, D. J. *J. Phys. C* **1976**, *9*, 2481.
(15) McClure, D. S. In Optical Properties of Ions in Solids; di Bartolo, B., Ed.; Plenum: New York, 1974.

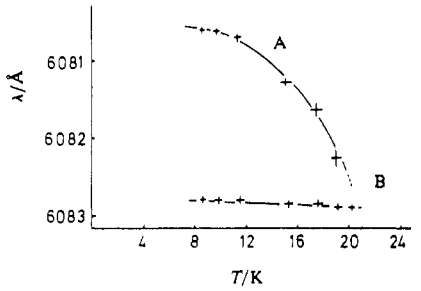

Figure 3. Temperature variation of the wavelengths of absorption bands A and B.[16]

halides such absorption bands are usually about 50–100 cm^{-1} wide, corresponding to the energy difference between the Brillouin zone center and zone edge magnons of zJ_nS, where z is the number of (n) neighbors, J_n is the exchange constant, and S is the spin. However, in Figure 2, one can see that the "cold" bands are very much narrower, suggesting that they arise from coupling between the exciton and a magnetic fluctuation that only has a very weak dispersion. The alternative explanation, that the bands corresponded to absorption by creating the exciton alone, could be ruled out by their polarization.

Although it is difficult to polish the mica-like crystals perpendicular to the easy cleavage plane, we measured polarized spectra with the incident light parallel and perpendicular to the layers. We found that they were allowed by the electric-dipole mechanism, like the nearby hot exciton–magnon combination, rather than magnetic-dipole, as expected if they were pure exciton lines. Another unusual feature is that the separation between the cold bands changes with temperature; in fact the most intense one remains almost fixed while the weaker one moves toward it as the temperature rises (Figure 3). Extrapolating, the temperature at which they would both have the same energy turns out to be that where their intensities both tend to zero, i.e., about 23 K.

That the two sharp cold bands signal a peculiarity in the magnetic structure is strongly indicated by their behavior when a magnetic field is applied.[14,16] In fields applied perpendicular to the layers the bands are almost unaffected, except for a small shift to higher frequency that only starts to become appreciable above 10 T. (Measurements in such high fields, up to 15 T, were made with a pulsed magnet.) Contrastingly, with the field parallel to the layers there is a dramatic effect: the bands remain unchanged up to a critical value of the field H_c at which they vanish sharply. H_c is also a function of temperature, decreasing from 2.7 T at 4 K smoothly toward zero at 23 K (Figure 4). Figure 4 therefore defines a phase diagram in the H,T plane and delineates the existence region of a magnetic phase that we have labeled A_2. But what is it? The method of choice for determining magnetic structures is neutron diffraction, so it was to this that we turned next.

Neutron Diffraction

Single-crystal neutron diffraction measurements[14,17] showed that below its Neel temperature of 52 K, $NiBr_2$ adopts a magnetic structure in which the $S = 1$ ($3d^8$)

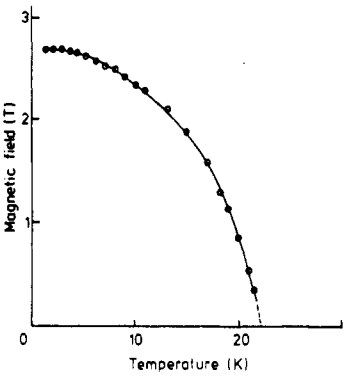

Figure 4. Temperature variation of the critical field at which bands A and B (Figure 3) disappear.[14]

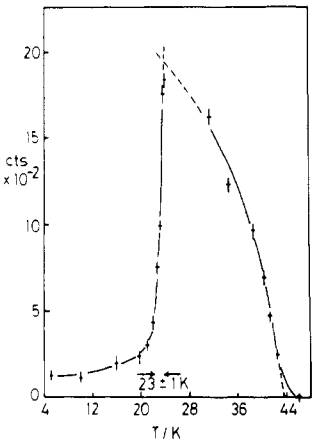

Figure 5. Temperature dependence of the maximum scattered neutron intensity at (003/2) in $Ni_{0.94}Fe_{0.06}Br_2$.[18]

moments localized on each Ni^{2+} lie parallel to one another within the planes of the layers, with alternate layers being antiparallel. That is, ferromagnetic layers are weakly coupled antiferromagnetically as in the other MX_2 halides. In the rhombohedral (D^5_{3d}) space group of the $CdCl_2$ crystal structure, (00l) nuclear Bragg reflections are allowed for $l = 3n$. The antiferromagnetic order between the planes perpendicular to the c axis doubles the unit cell along this axis below 52 K, and magnetic Bragg reflections (003/2), (005/2), etc. are observed with intensities that increase with decreasing temperature following the spontaneous magnetization (Figure 5). Below 23 K, however, a remarkable change occurs, and the intensity at (003/2) suddenly drops. Where has it gone?

With a classical single-detector diffractometer, such as D15 at the high-flux beam reactor of the Institut Laue-Langevin (ILL), Grenoble, France, the most convenient way to monitor the intensity in the neighborhood of (003/2) as a function of temperature is by setting the neutron detector to the Bragg angle 2θ, corresponding to the center of the reflection, and rocking the crystal angle ω with the c axis in the horizontal plane. In that way we found that below 23 K the reflection broadens and splits into two satellite peaks that shift smoothly with decreasing temperature as shown in Figure 6 for a crystal doped with a small concentration of Fe^{2+}.[18] The magnetic Bragg intensity no longer peaks at (003/2), but at ($\delta\delta$3/2), where δ reaches a limiting value of 0.027 at 4 K. This means that within the layers the spins are no longer parallel

(16) Moore, M. W.; Wood, T. E.; Day, P. *J. Chem. Soc.*, Faraday Trans 2, **1981**, *77*, 1611.
(17) Day, P.; Ziebeck, K. R. A. *J. Phys. C* **1980**, *13*, L523.
(18) Moore, M. W.; Day, P. *J. Solid State Chem.* **1985**, *59*, 23.

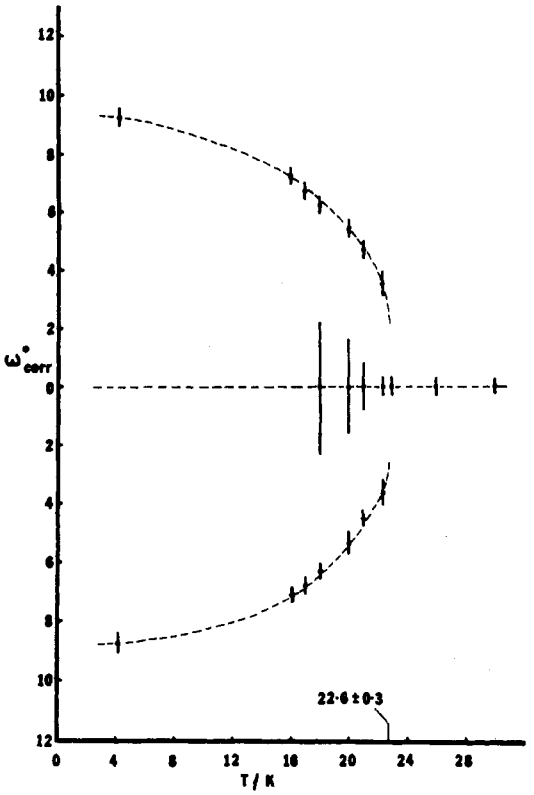

Figure 6. Temperature dependence of the separation ω°_{corr} in crystal angle between the magnetic satellite neutron diffraction peaks around (003/2) in $Ni_{0.99}Fe_{0.01}Br_2$.[18]

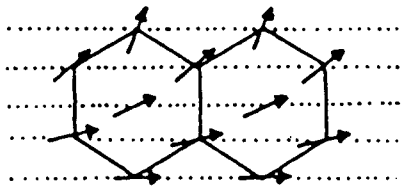

Figure 7. Helical arrangement of spins in the basal plane of $NiBr_2$.

but that a new repeat distance of δ^{-1} has become established. Careful searching for higher order reflections ($n\delta$, $n\delta$, $^3/_2$) revealed none, so the arrangement of the moment vectors along (110) is sinusoidal. Another way of putting it is that the moments in each plane perpendicular to (110) are all parallel, but that on passing from each layer to the next there is a turn angle of $\pi\delta$, or about 5°, thus describing a helix (Figure 7).

To make quite sure that the direction of the helix is along (110) and that there are no other satellite peaks, one should scan over all crystal and scattering angles or, put in other words, search the whole region of the reciprocal lattice around (003/2), a tedious undertaking with a single-detector diffractometer that has to step and count through successive small solid angles. Fortunately, multidetectors for neutrons are now becoming available, thus permitting simultaneous counting at many reciprocal lattice points. For example, the D16 diffractometer at ILL has a ^3He detector containing 64 × 16 elements, subtending a maximum total angle of some 10° about the sample. With this instrument one can set the angle of the crystal and get good counting statistics for a mesh of 1024 reciprocal lattice points in about 5–10 min. Stepping the crystal angle and repeating the count, one may quickly search a large volume of reciprocal space.[19] The result is shown as a contour diagram in Figure 8a.

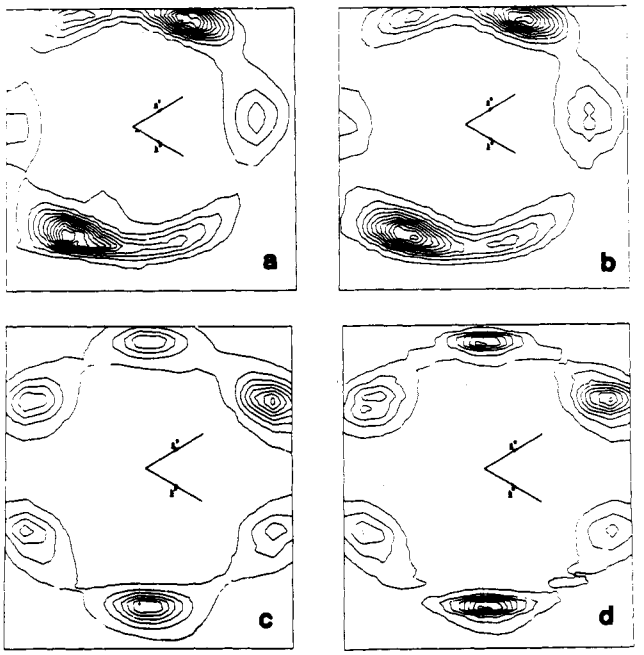

Figure 8. Neutron scattering intensity contours of magnetic satellites around (003/2): (a, b) $NiBr_2$, observed and simulated; (c, d) $Ni_{0.91}Fe_{0.09}Br_2$, observed and simulated.[19]

There are six satellite peaks forming a regular hexagon because in the absence of an applied magnetic field there are three equivalent spin orientations, along (110), ($\bar{1}10$), and ($1\bar{1}0$). Actually the three pairs of satellites in Figure 8a do not have equal intensities, probably because the crystal was slightly strained on mounting. Above 23 K, the temperature of the incommensurate–commensurate transition T_{IC}, the hexagon vanishes and is replaced by a single peak centered at (003/2). Since only the temperature is changed, and the mosaic spread of the crystal and the resolution of the diffractometer remain the same, we can safely assume that the shape of the single (003/2) peak arising in the commensurate phase is the same as that of each of the ($\delta\delta$3/2) satellites in the incommensurate phase. Without making any assumptions about how many pairs of satellites there are, we can model the total intensity by placing pairs of peaks around a ring of radius δ, varying their number and relative intensity to optimize the fit. The result of this procedure (Figure 8b) is in excellent agreement with the observed profile.

Our conclusion from neutron diffraction is therefore that from 52 to 23 K $NiBr_2$ has a collinear easy plane metamagnetic structure, but that at 23 K the spins begin to cant about the (110) direction, so that the angle between successive spins increases smoothly from zero to a maximum of about 5°. So far as is known, such behavior is unique among nonmetallic compounds. Why does $NiBr_2$ do it?

The Magnetic Phase Diagram

Superimposed on the layer structure in Figure 1B are the three types of near neighbors. In common with the other MX_2 having predominantly 90° superexchange pathways between the nearest neighbors, the J_n in $NiBr_2$ should be ferromagnetic. If J_{nn} and J_{nnn} are antiferromagnetic, however, the ground state could be

(19) Day, P.; Moore, M. W.; Wilkinson, C.; Ziebeck, K. R. A. *J. Magn. Magn. Mater.* **1985**, *50*, 1.

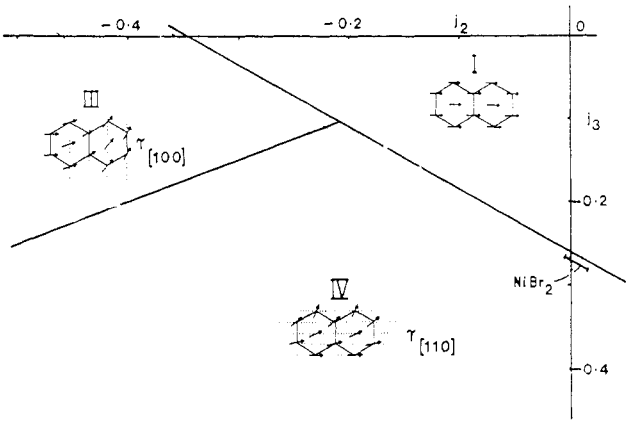

Figure 9. Calculated phase diagram for a planar hexagonal Heisenberg antiferromagnetic.[20] Phase II (not shown) is collinear antiferromagnetic.

a canted one. Some years ago Rastelli et al.[20] calculated the phase diagram for a planar triangular lattice as a function of $j_i = z_i J_i / z_n J_n$, where i represents (nn) and (nnn), with the result shown in Figure 9. Clearly, when j_{nn} and j_{nnn} are both positive, the lattice is ferromagnetic, but when either or both are negative, helical or antiferromagnetic phases are predicted. $NiBr_2$ lies within phase IV of Figure 9. To find the experimental values of the J_i, inelastic neutron scattering was carried out by using long-wavelength neutrons to concentrate on the lowest energy part of the magnon dispersion.[21] We found that J_{nn} was zero within experimental error but that J_{nnn} was indeed negative, placing $NiBr_2$ just inside phase IV, but very close to the boundary of the collinear phase I.

The helical magnetic structure found in $NiBr_2$ at low temperature results from a very delicate and fortuitous balance of the various J_i. Raising the temperature forces the system across the boundary from phase IV to phase I. To see whether this was the result of lattice expansion altering J_n, we performed single-crystal neutron diffraction as a function of hydrostatic pressure.[22] The result was suprising: δ decreases with increase of pressure, just as it does with increasing temperature, so the temperature-induced transition is not due to lattice expansion. The theorists' belief at the moment is that thermally excited spin fluctuations change the effective values of J_i.[23]

Chemical Substitution

Given the extreme sensitivity of the magnetic structure to J_{nn} and J_{nnn}, chemical substitution should have some interesting effects. $NiCl_2$ is collinear (phase I, Figure 9) at all temperatures,[24] and NiI_2 has a temperature-independent helical structure,[25] though in neither case are j_{nn} and j_{nnn} known. Doping $NiBr_2$ with Cl^- rapidly reduces both δ and T_{IC} until above 10% substitution, no helical phase is seen.[26] Conversely, I^- increases both δ and T_{IC}.[27] Diluting the moments by substituting 8% Zn^{2+} for Ni^{2+} has virtually no effect on δ and only slightly reduces T_{IC}, but an exploration of the magnetic satellite structure around (003/2) showed that there was no longer any preferred direction of the helix within the layers. Instead of a hexagon of satellite peaks as in Figure 8, the scattering contours were fitted best by a ring.[28] Equally remarkable is the effect of Fe^{2+}.[28] In $FeBr_2$ itself the moments lie parallel to the c axis, i.e., orthogonal to the Ni^{2+} moments in $NiBr_2$. Up to 3% Fe^{2+} doping, the $NiBr_2$ magnetic structure is unaffected, both as to T_{IC} and the magnitude and direction of δ. However, doping between 3 and 9% Fe^{2+} changes the direction of the helix from (110) to (100), although δ still has the same magnitude. This can be seen from the rotation of the satellite hexagon (Figure 8c,d).[19] We have thus passed from phase IV to III. Above 9% Fe^{2+} the entire magnetic structure changes over the easy axis structure of $FeBr_2$ itself, because of the strong axial anisotropy of Fe^{2+} in this lattice geometry. The x,T phase diagram of $Ni_{1-x}Fe_xBr_2$ is shown in Figure 10.

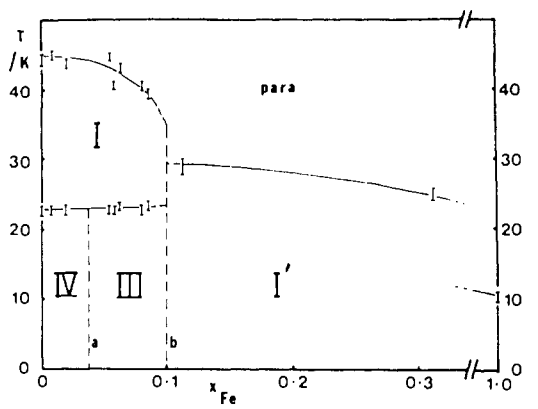

Figure 10. Observed magnetic phase diagram of $Ni_{1-x}Fe_xBr_2$ from neutron diffraction.[18] The Roman numerals correspond to Figure 9.

Conclusion

This Account has described how a combination of optical spectroscopy and neutron scattering, combined with chemical substitution, has led to a better understanding of the unique magnetic behavior of $NiBr_2$. Structurally it is a very simple compound, but a delicate balance of competing ferro- and antiferromagnetic interactions produces a gamut of strange magnetic behavior.

Our group has been supported by the UK SERC, and access to neutron beams was provided by AERE Harwell and ILL Grenoble.

(20) Rastelli, E.; Tassi, A.; Reatto, L. *Physica B*, **1979**, *97B*, 1.
(21) Day, P.; Moore, M. W.; Wood, T. E.; Paul, D. Mc.; Ziebeck, K. R. A.; Regnault, L. P.; Rossat-Mignod, J. *Solid State Commun.* **1984**, *51*, 627.
(22) Day, P.; Vettier, C. *J. Phys. C* **1981**, *17*, L195.
(23) Rastelli, E.; Tassi, A. *J. Magn. Magn. Mater.* **1986**, *54–57*, 1147.
(24) Lindgard, P. A.; Birgeneau, R. J.; Als-Neilsen, J.; Guggenheim, H. J. *J. Phys. C* **1975**, *8*, 1059.
(25) Kuindersma, S. R.; Sanchez, J. P.; Haas, C. *Physica B* **1981**, *111B*, 231.
(26) Day, P.; Turner, K.; Visser, D.; Wood, T. E. *Phys. Status Solidi B* **1982**, *113*, 623.
(27) Moore, M. W.; Day, P.; Wilkinson, C.; Ziebeck, K. R. A. *Solid State Commun.* **1985**, *53*, 1009.
(28) Day, P.; Moore, M. W.; Wilkinson, C.; Ziebeck, K. R. A. *J. Phys. C* **1981**, *14*, 3423.